

Color image analysis via Racah moments

Yexiao Wu, Simon Liao

Department of Applied Computer Science, The University of Winnipeg, Canada

jane.yexiao.wu@gmail.com, s.liao@uwinnipeg.ca

Abstract: *In this research, Racah moments color image descriptors are investigated. Channels separation for color images were involved in RGB color space, and Racah moments from each channel were computed individually. In experiments, we have performed the color image reconstructions from different color channels and various orders of Racah moments. Our experimental results have demonstrated that, by applying Racah moments, color images can be completely reconstructed without any information loss. We have also discovered that the individual set of Racah moments will uniquely describe the color image features, while the lower and higher orders of Racah moments will preserve more of features from the bottom right and top left regions of a color image, respectively.*

Keywords: *Racah moments, color image reconstruction*

1. Introduction

In our daily life, we could easily be benefited from color images as a widely used information medium, which are capable of directly recording complex details.

The moment method applied in the image representation was first introduced by Hu [4] in 1962. Since then, the moment descriptors have been investigated and applied in various scientific fields, such as image analysis and invariant pattern recognition [5, 6, 3].

The discrete orthogonal moments based on Tchebichef and Krawtchouk polynomials were first introduced by Mukundan et al. [9] and Yap et al. [7] in 2001 and 2003, respectively. The appearance of the discrete orthogonal moments, which are justified if the function of interest is represented in the form of tabulated values, has considerably enriched the moment methods. Image analysis by discrete orthogonal Racah moments was proposed by Zhu et al. [16]. With some satisfied performances in the tasks of image analysis and recognitions, the Racah moment-based features have been utilized in a Chinese character recognition system in 2014 [12].

The moment-based color image features have also been investigated and applied in the field of image analysis. The traditional approach to achieve the color image analysis is to separate a color image into three channels first, and then extract moment features individually from the three color component channels [14, 2, 1, 11, 15].

In this research, we have investigated the capabilities of discrete orthogonal Racah moment feature representations from the aspect of color images. We have performed the color image reconstructions from Racah moments by decomposing a color image into three channels and extract moment features separately. We have also conducted a study on the ability to describe the color image features by individual set of Racah moments.

The rest of the paper is organized as follows. Section 2 will briefly introduce Racah moments and its computation. Section 3 presents the experimental results and analysis on color image reconstructions. Finally, the concluding remarks are given in Section 4.

2. Racah moments and computing

The $n + m$ th order of Racah moments describe a testing image $f(x, y)$ size of $N \times N$ pixels as [16]

$$U_{nm} = \sum_{s=a}^{b-1} \sum_{t=a}^{b-1} U_n^{(\alpha, \beta)}(s, a, b) U_m^{(\alpha, \beta)}(t, a, b) f(x, y), \quad (1)$$

$$n, m = 0, 1, \dots, N - 1, x = s - a + 1, y = t - a + 1,$$

where (x, y) denotes the pixel positions in an image function. $U_n^{(\alpha, \beta)}(s, a, b)$ is the weighted Racah polynomials [16]

$$U_n^{(\alpha, \beta)}(s, a, b) = u_n^{(\alpha, \beta)}(s, a, b) \sqrt{\frac{\rho(s)}{d_n^2} [\Delta x(s - \frac{1}{2})]}, \quad (2)$$

where

$$\rho(s) = \frac{(a + s)!(-a + \beta + s)!(\alpha + b - s - 1)!(\alpha + b + s)!}{(s - a)!(b - s - 1)!(b + s)!(a - \beta + s)!}, \quad (3)$$

$$x(s) = s(s + 1), \quad (4)$$

$$d_n^2 = \frac{\Gamma(\alpha + n + 1) \Gamma(\beta + n + 1) \Gamma(b - a + \alpha + \beta + n + 1)}{(\alpha + \beta + 2n + 1) n! (b - a - n - 1)! \Gamma(\alpha + \beta + n + 1)} \times \frac{\Gamma(a + b + \alpha + n + 1)}{\Gamma(a + b - \beta - n)}. \quad (5)$$

$u_n^{(\alpha, \beta)}(s, a, b)$ is the n th order classical Racah polynomial given by [16]

$$u_n^{(\alpha, \beta)}(s, a, b) = \frac{1}{n!} (a - b + 1)_n (\beta + 1)_n (a + b + \alpha + 1)_n \times {}_4F_3(S), \quad (6)$$

in which,

$$(u)_k = u(u + 1) \cdots (u + k - 1) = \frac{\Gamma(u + k)}{\Gamma(u)}, \quad (7)$$

$${}_4F_3(a_1, a_2, a_3, a_4; b_1, b_2, b_3; z) = \sum_{k=0}^{\infty} \frac{(a_1)_k (a_2)_k (a_3)_k (a_4)_k}{(b_1)_k (b_2)_k (b_3)_k} \frac{z^k}{k!}, \quad (8)$$

and S represents

$$\left(\begin{matrix} -n, \alpha + \beta + n + 1, a - s, a + s + 1 \\ \beta + 1, a + 1 - b, a + b + \alpha + 1 \end{matrix} ; 1 \right). \quad (9)$$

Image can be reconstructed by the inverse Racah moments transform

$$f(x, y) = \sum_{n=0}^{N-1} \sum_{m=0}^{N-1} U_{nm} U_n^{(\alpha, \beta)}(s, a, b) U_m^{(\alpha, \beta)}(t, a, b), \quad (10)$$

$$s, t = a, a + 1, \dots, b - 1, x = s - a + 1, y = t - a + 1.$$

One can refer to [13] for more details.

In terms of RGB color images $f(s, t)$, it can be divided into red, green and blue components. Therefore, $N \times N$ color image $f(s, t)$ can be represented as

$$f(s, t) = [f_R(s, t), f_G(s, t), f_B(s, t)], \quad s, t = 1, 2, \dots, N \quad (11)$$

where $f_R(s, t)$, $f_G(s, t)$, and $f_B(s, t)$, are the red, green and blue components of the image pixels, respectively.

Then, Racah moments of $N \times N$ multi-channel images with order $n + m$ is defined as

$$\begin{aligned} U_{nm} = & \\ & \left[\sum_{s=a}^{b-1} \sum_{t=a}^{b-1} U_n^{(\alpha, \beta)}(s, a, b) U_m^{(\alpha, \beta)}(t, a, b) f_R(s - a + 1, t - a + 1), \right. \\ & \sum_{s=a}^{b-1} \sum_{t=a}^{b-1} U_n^{(\alpha, \beta)}(s, a, b) U_m^{(\alpha, \beta)}(t, a, b) f_G(s - a + 1, t - a + 1), \\ & \left. \sum_{s=a}^{b-1} \sum_{t=a}^{b-1} U_n^{(\alpha, \beta)}(s, a, b) U_m^{(\alpha, \beta)}(t, a, b) f_B(s - a + 1, t - a + 1) \right]. \end{aligned} \quad (12)$$

Color image reconstructions can be performed by inverse transformation

$$\begin{aligned} f(s - a + 1, t - a + 1) = & \\ & \left[\sum_{n=0}^M \sum_{m=0}^M U_{R, nm} U_n^{(\alpha, \beta)}(s, a, b) U_m^{(\alpha, \beta)}(t, a, b), \right. \\ & \sum_{n=0}^M \sum_{m=0}^M U_{G, nm} U_n^{(\alpha, \beta)}(s, a, b) U_m^{(\alpha, \beta)}(t, a, b), \\ & \left. \sum_{n=0}^M \sum_{m=0}^M U_{B, nm} U_n^{(\alpha, \beta)}(s, a, b) U_m^{(\alpha, \beta)}(t, a, b) \right]. \end{aligned} \quad (13)$$

where $U_{R, nm}$, $U_{G, nm}$, and $U_{B, nm}$, are the red, green and blue Racah moments of each channel.

The weighted Racah polynomials has recurrence relation with respect to n [16]

$$A_n U_n^{(\alpha, \beta)}(s, a, b) = B_n \frac{d_{n-1}}{d_n} U_{n-1}^{(\alpha, \beta)}(s, a, b) + C_n \frac{d_{n-2}}{d_n} U_{n-2}^{(\alpha, \beta)}(s, a, b), \quad (14)$$

where

$$A_n = \frac{n(\alpha + \beta + n)}{(\alpha + \beta + 2n - 1)(\alpha + \beta + 2n)}, \quad (15)$$

$$\begin{aligned} B_n = & x - \frac{a^2 + (a - \beta)^2 + b^2 + (\alpha + b)^2 - 2}{4} \\ & + \frac{(\alpha + \beta + 2n - 2)(\alpha + \beta + 2n)}{8} - \frac{(\beta^2 - \alpha^2) \left(\left(\frac{\alpha}{2} + b \right)^2 - \left(a - \frac{\beta}{2} \right)^2 \right)}{2(\alpha + \beta + 2n - 2)(\alpha + \beta + 2n)}, \end{aligned} \quad (16)$$

$$C_n = -\frac{(\alpha + n - 1)(\beta + n - 1)}{(\alpha + \beta + 2n - 2)(\alpha + \beta + 2n - 1)} \times$$

$$\left[\left(\frac{\alpha - \beta}{2} + a + b \right)^2 - \left(\frac{\alpha + \beta}{2} + n - 1 \right)^2 \right] \times$$

$$\left[\left(\frac{\alpha + \beta}{2} - a + b \right)^2 - \left(\frac{\alpha + \beta}{2} + n - 1 \right)^2 \right], \quad (17)$$

and

$$U_0^{(\alpha, \beta)}(s, a, b) = \sqrt{\frac{(2s + 1)\rho(s)}{d_0^2}}, \quad (18)$$

$$U_1^{(\alpha, \beta)}(s, a, b) = \frac{1}{\rho(s)} \frac{\rho_1(s) - \rho_1(s-1)}{x(s+1/2) - x(s-1/2)} \sqrt{\frac{(2s+1)\rho(s)}{d_1^2}}. \quad (19)$$

The recurrence relation with respect to s of weighted Racah polynomials is [16]

$$U_n^{(\alpha, \beta)}(s, a, b) = W \sqrt{\frac{\rho(s)(2s+1)}{\rho(s-1)(2s-1)}} U_n^{(\alpha, \beta)}(s-1, a, b)$$

$$- Z \sqrt{\frac{\rho(s)(2s+1)}{\rho(s-2)(2s-3)}} U_n^{(\alpha, \beta)}(s-2, a, b), \quad (20)$$

with

$$W = \frac{(2s-1)[\sigma(s-1) + (s-1)\tau(s-1) - 2\lambda s(s-1)]}{(s-1)[\sigma(s-1) + (2s-1)\tau(s-1)]}, \quad (21)$$

$$Z = \frac{s\sigma(s-1)}{(s-1)[\sigma(s-1) + (2s-1)\tau(s-1)]}, \quad (22)$$

and

$$U_n^{(\alpha, \beta)}(0, a, b) = \frac{1}{n^2} (a+n)(\beta-a+n)(b+\alpha+n)(b-n) \frac{d_{n-1}}{d_n} U_{n-1}^{(\alpha, \beta)}(0, a, b), \quad (23)$$

$$U_n^{(\alpha, \beta)}(1, a, b) = \frac{2}{(n+2)(n+1)\rho(1)} \left[\frac{\rho_n(1)}{\rho_n(0)} - \frac{n(n+1)}{2} \right] \sqrt{\frac{3\rho(1)}{\rho(0)}} U_n^{(\alpha, \beta)}(0, a, b), \quad (24)$$

in which,

$$\rho_n(s) = \rho(n+s) \prod_{k=1}^n \sigma(k+s), \quad (25)$$

$$\sigma(s) = (s-a)(b+s)(a-\beta+s)(\alpha+b-s), \quad (26)$$

$$\tau(s) = (\alpha+1)a(a-\beta) - (\alpha+1)(\beta+1) + b(\beta+1)$$

$$(\alpha+b) - s(s+1)(\alpha+\beta+2), \quad (27)$$

$$\lambda_n = n(\alpha + \beta + n + 1). \quad (28)$$

3. Color image reconstructions from Racah moments

In this section, we will present the experimental results of color images reconstructions from Racah moments. To process a color image, we can separate the original color image into three primary colors, red (R), green (G), and blue (B), and use the values of the three colors to measure the color intensity of a pixel.

In our experiments, we will firstly separate an original color image into three image channels in RGB color space, and then compute the Racah moments and perform the image reconstructions in three image channels separately. Finally, we combine the three reconstructed channel images into one color image and evaluate the quality of the reconstructed color image from Racah moments.

To assess the image reconstruction performances, we use the Mean Square Error (MSE) and Peak Signal to Noise Ratio (PSNR) to measure the qualities of the reconstructed images. The Mean Square Error between a reconstructed image and its original image is defined as

$$MSE = \frac{1}{N^2} \sum_{i=1}^N \sum_{j=1}^N [f(x_i, y_j) - \hat{f}(x_i, y_j)]^2, \quad (29)$$

where $f(x_i, y_j)$ denotes the original image and $\hat{f}(x_i, y_j)$ is its reconstructed version.

The Peak Signal to Noise Ratio represents the ratio of the maximum power of the signal to the affecting noise

$$PSNR = 10 \log_{10} \left(\frac{G_{Max}^2}{MSE} \right), \quad (30)$$

where G_{Max} is the maximum image intensity value of the original image. The MSE value of a color image is the average MSE values of the three color components.

We have utilized the three color images shown in the first column of Fig. 1 as our testing images, which have 256 image intensity values, are sized at 128×128 , and are named as Image1, Image2, and Image3, respectively. Images displayed in the columns two, three, and four of Fig. 1 are the red(R), green(G), and blue(B) components of the original color image shown in the first column of the same row.

We have performed the image reconstructions on the three original color images shown in Fig. 1 from Racah moments with different maximum orders up to $n = m = 127$. Fig. 2 shows some of the reconstructed color images of all three original testing images from applying different orders of Racah moments. It can be observed that the results of color image reconstruction will be improved when the orders of Racah moments go higher.

Table 1 displays the MSE and PSNR values of the reconstructed original color image Image1, shown in the first row of Fig. 1, from applying different orders of Racah moments. The MSE and PSNR values presented in the bottom line of Table 1 indicates that when the order of Racah moments reaches $n = m = 127$, the color image is reconstructed completed without any error. This also suggests that the Racah moments computational approach adopted in this research is very accurate.

Fig. 3 plots the MSE values of the reconstructed three color components of the testing image, Image1, shown in Fig. 1. It can be noticed that, for the same order of Racah moments, the blue channel always has the best reconstruction performance with the lowest MSE value, while the green component produces the highest MSE.

Table 2 presents the MSE and PSNR values of the reconstructed original color image, shown in the first column of the second row in Fig. 1, from using different orders of Racah

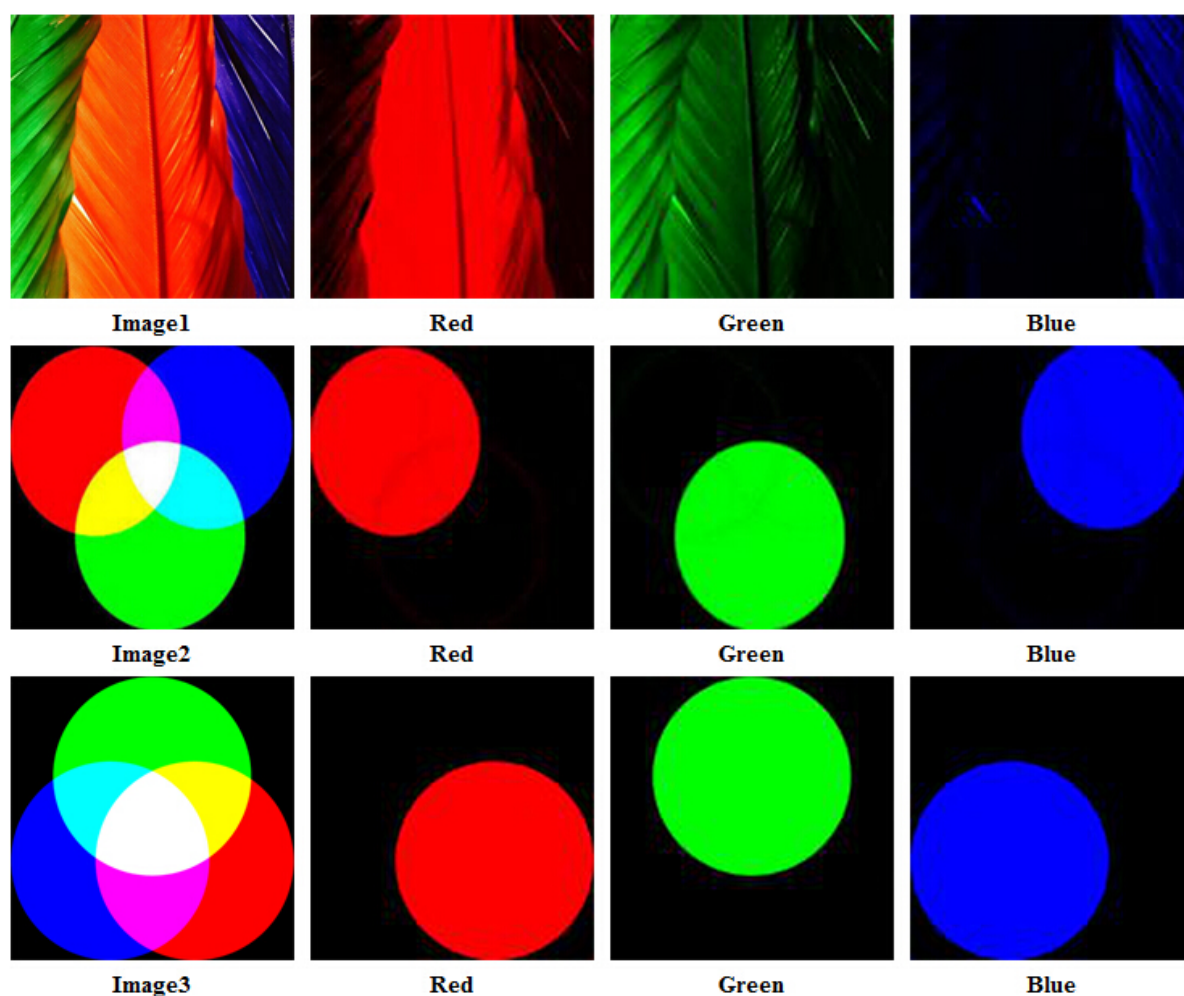


Figure 1. Columns 1 to 4 show the original images and their red, green, and blue components, respectively

Table 1. MSE and PSNR values of the reconstructed three channels images from original Image1

Order $n = m$	MSE			PSNR		
	Red	Green	Blue	Red	Green	Blue
9	1129.83	1175.99	547.63	17.60	17.42	20.74
30	417.24	432.31	201.00	21.92	21.77	25.09
50	197.44	228.50	98.77	25.17	24.54	28.18
70	97.24	124.13	46.55	28.25	27.19	31.45
100	24.09	33.52	11.84	34.31	32.87	37.39
120	5.05	6.11	2.16	41.09	40.27	44.76
127	0	0	0	∞	∞	∞

moments. The same as the results shown in Table 1, the original image is perfectly reconstructed when the order of Racah moments is $n = m = 127$.

Fig. 4 shows the plotting of the MSE values of the reconstructed three color components of the original testing image, Image2. In this experiment, the green channel is the best reconstructed and the red component has the highest MSE, though the differences are not as

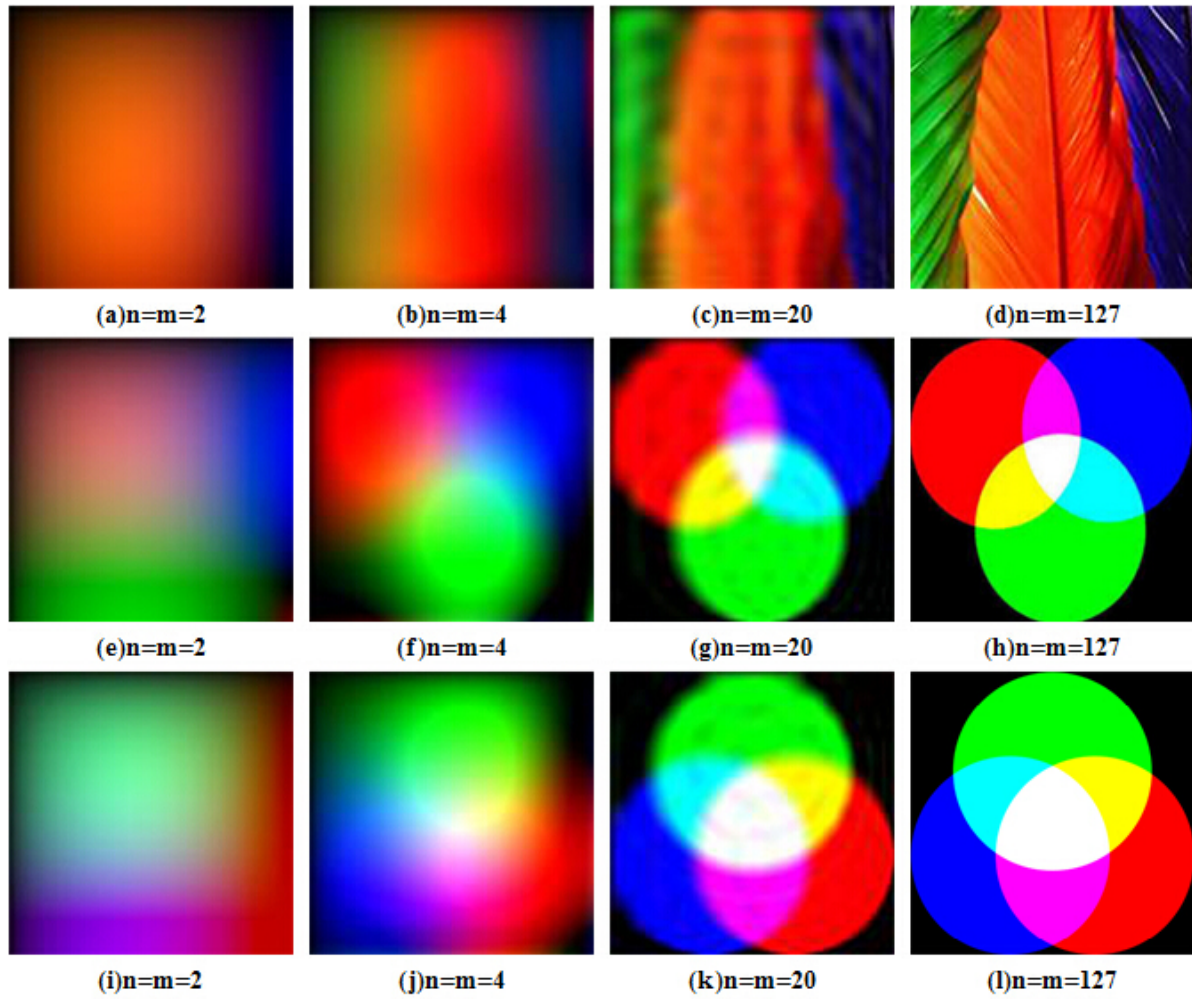


Figure 2. Reconstructed RGB images from Racah moments with different maximum orders

Table 2. MSE and PSNR values of the reconstructed three channels images from original Image2

Order	MSE			PSNR		
	Red	Green	Blue	Red	Green	Blue
10	1004.75	962.21	920.12	18.11	18.29	18.49
30	239.31	203.84	193.55	24.34	25.03	25.26
50	95.33	76.74	82.35	28.33	29.28	28.97
70	41.2	29.28	36	31.98	33.46	32.56
90	15.15	10.9	13.16	36.32	37.75	36.93
110	4.02	2.66	3.19	42.08	43.87	43.09
125	0.55	0.03	0.4	50.66	62.47	52
126	0.25	0	0.13	52.03	∞	56.78
127	0	0	0	∞	∞	∞

significant as those of Fig. 3. The smaller figure placed inside Fig. 4 highlights the differences among three reconstructed color components for higher Racah moments orders.

Table 3 displays the MSE and PSNR values of the reconstructed original color image, Image3, shown in the first column of the third row in Fig. 1, from applying different orders

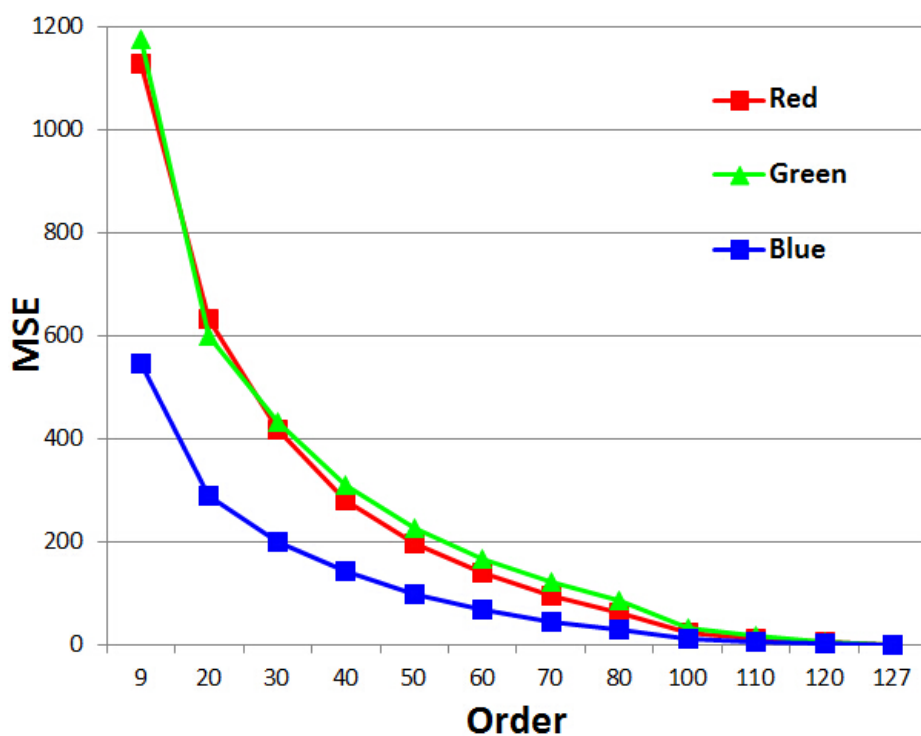


Figure 3. MSE values comparison of the reconstructed three color components from the original Image1

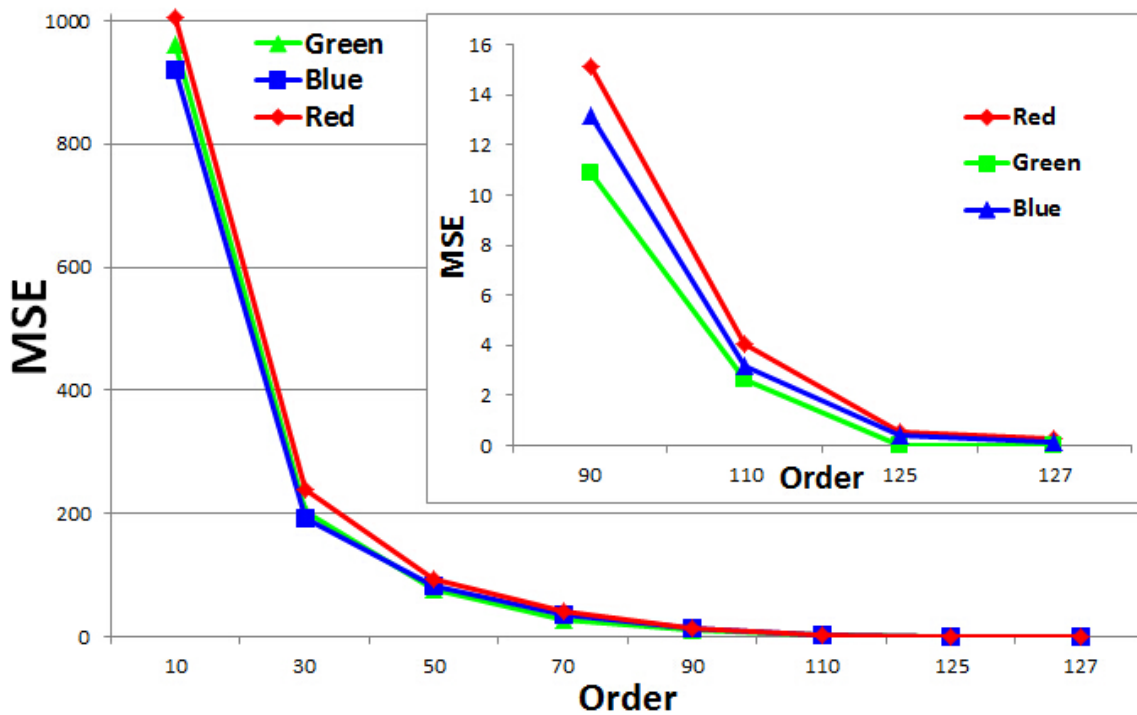


Figure 4. MSE values comparison of the reconstructed three color components from the original Image2

Table 3. MSE and PSNR values of the reconstructed three channels images from original Image3

Order	MSE			PSNR		
	Red	Green	Blue	Red	Green	Blue
10	922.22	1097.97	1029.16	18.48	17.72	18.00
30	220.97	297.73	268.16	24.68	23.39	23.84
50	92.46	126.94	116.31	28.47	27.09	27.47
70	43.84	57.69	54.80	31.71	30.51	30.74
90	19.20	25.01	23.28	35.29	34.14	34.46
125	0	14.46	1.04	∞	46.46	47.93
126	0	0.40	0.46	∞	52.04	51.42
127	0	0	0	∞	∞	∞

of Racah moments. As expected, the image reconstruction is completely achieved when the order of Racah moments reaches $n = m = 127$.

Fig. 5 demonstrates the plotting of the MSE values of the three color components reconstructed from the original testing image, Image3. In this experiment, the red channel is the best reconstructed color and the green component has the highest MSE. It should be noted that the result shown in Fig. 5 contrast to that of Fig. 4. The figure displayed inside Fig. 5 focuses the differences of three reconstructed color components when the orders of Racah moments are higher than 70.

To observe the three original testing color images, Image1, Image2, Image3, and the MSE values of the reconstructed three color components of all three testing images shown in Fig 3,

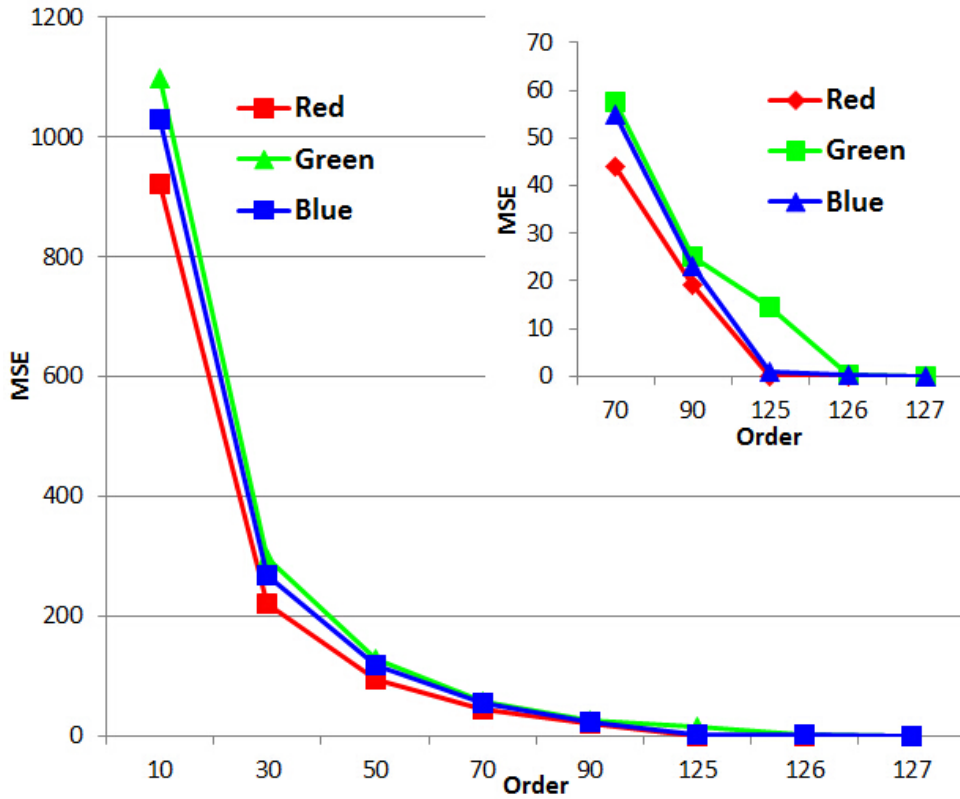


Figure 5. MSE values comparison of the reconstructed three color components from the original Image3

Fig 4, and Fig 5, we can find that when the orders of Racah moments are lower, the colors located around the bottom right region of an image will be more noticeably reconstructed. When the orders of Racah moments go higher, the reconstruction performances around the bottom right region will always be improved ahead those of top left region.

These observations lead to the conclusion that the lower orders of Racah moments contain more color image information of the bottom right region of an image, while the higher orders of Racah moments represent more image features in the top left region.

4. Concluding remarks

In this research, we have investigated the image feature representative capabilities of Racah moment from the aspect of color image reconstruction. Our experimental results have demonstrated that Racah moments have a satisfying performance on color image reconstructions, which can perfectly reconstruct a color image when the maximum order of Racah moments is one less than the size of the image.

We have also discovered that each individual set of Racah moments will uniquely and independently describe the color image features. The lower orders of Racah moments will preserve more of image information from the bottom right region of a color image, while the higher orders of Racah moments will represent the features in the top left region more.

References

- [1] L.V. Gool F. Mindru, T. Tuytelaars and T. Moons. Moment invariants for recognition under changing viewpoint and illumination. *Comput. Vis. Image Und.*, pages 3–27, 2004.
- [2] T. Moons F. Mindru and L.V. Gool. Color-based moment invariants for the viewpoint and illumination independent recognition of planar color patterns. *In Int. Conf. Advances in Pattern Recognition (ICAPR'98)*, pages 113–122, 1998.
- [3] J. Flusser, T. Suk, and B. Zitova. *Moments and moment invariants in pattern recognition*. John Wiley & Sons, Ltd, 2009.
- [4] M. K. Hu. Visual pattern recognition by moment invariants. *IRE Transactions on Information Theory*, 8:179–187, 1962.
- [5] R. Mukundan and K.R. Ramakrishnan. *Moment Functions in Image Analysis - Theory and Applications*. World Scientific, 1998.
- [6] M. Pawlak. *Image Analysis by Moments: Reconstruction and Computational Aspects*. Oficyna Wydawnicza Politechniki WrocLawskiej, WrocLaw, 2006.
- [7] Y. Pew-Thian, P. Raveendran, and O. Seng-Huat. Image analysis by krawtchouk moments. *Image Processing, IEEE Transactions on*, 12(11):1367–1377, 2003.
- [8] S. H. Ong R. Mukundan and P. A. Lee. Discrete vs. continuous orthogonal moments for image analysis. *International. Conf. on Imaging Science, Systems and Technology-CISST'01*, pages 23–29, 2001.
- [9] M. Ramakrishnan, O. SH, and L. Poh Aun. Image analysis by tchebichef moments. *Image Processing, IEEE Transactions on*, 10(9):1357–1364, 2001.
- [10] S. J. Sangwine. Fourier transforms of colour images using quaternion or hypercomplex numbers. *Electron, Lett.*, pages 1979–1980, 1996.
- [11] T. Suk and J. Flusser. Affine moment invariants of color images. *In CAIP 2009, LNCS5702*, pages 334–341, 2009.
- [12] Y. Wu and S. Liao. Chinese characters recognition via racah moments. *Audio, Language and Image Processing (ICALIP)*, pages 691–694, 2014.

- [13] Y. Wu and S. Liao. Image reconstruction from racah moments. *Accepted by The 29th Annual IEEE Canadian Conference on Electrical and Computer Engineering (CCECE 2016)*, 2016.
- [14] C.C. Chang Y.K. Chan. A color image retrieval method based on color moment and color variance of adjacent pixels. *Int. J. Pattern Recognition. Artif. Intell.*, 16:113–125, 2002.
- [15] X. Zhang and S. Liao. Color image reconstruction from charlier moments. *Journal of Theoretical and Applied Computer Science*, page in press, 2016.
- [16] H. Zhu, H. Shu, J. Liang, L. Luo, , and J.-L. Coatrieux. Image analysis by discrete orthogonal racah moments. *Signal Processing*, 87(4):687–708, 2007.